Processing and Characterization of Iron oxide nanoparticle developed by mechanical grinding using a ball milling machine

ABSTRACT

In this study iron oxide (Fe_2O_3) nanoparticle samples was prepared using mechanical grinding method. The optical properties were studied using UV-Vis spectrophotometer within a range of 200-1100nm. The micro and crystalline size of the nanoparticle were studied using x-ray diffractometer (XRD) and scanning electron microscopy (SEM). The compositional analysis was carried out using energy dispersive x-ray spectroscopy (EDXS) and molar concentration of the elements was done using atomic absorption spectroscopy (AAS). Observation of the electrical properties of the nanoparticle was carried out using an electrical four-point probe system. The XRD pattern in the 2θ range from 20 to 70^0 revealed that iron oxide had a rhombohedral structure. The SEM result showed that the nanoparticles were well dispersed and had a uniform crystalline structure. The AAS results uncovered the concentration of iron in the nanoparticles that was processed. The concentration of iron was 17.336mg/l. The EDXS results showed the elemental analysis of the nanoparticles under consideration. Iron oxide nanoparticles had elemental composition of oxygen, iron, titanium and carbon. The atomic and weight concentration of iron was 14.19 and 30.89%. The four-point probe electrical resistivity result shows that iron oxide nanoparticles had a sheet resistance of $9.8x10^6\Omega$/sq. The optical result made it known that iron oxide nanoparticles possessed a high transmittance, also iron oxide nanoparticles displayed a low reflectance and moderate absorbance. Finally, the bandgap energy of Fe_2O_3 dispersed in ethanol was found to be 2.74 eV. The Band gap of Fe_2O_3 dispersed in distilled water is 2.98 eV.

Keywords: Fe_2O_3 nanoparticles, Absorbance, electrical resistivity.

1. INTRODUCTION

Advancement in science and technology has expanded the requirements for energy around the globe. The consequence is that many nations have resorted to reusable energy to match their demands. To this end nanoscale size of particle, particularly of oxide materials has made the field of material science more applied and fascinating area of research due to versatile application such as optoelectronics, photo-solar cells and so on. According to [1] nanoscience is

the study of matters property at a nanoscale. In nanotechnology particle size is less than 100nm and the appearance of new behavior that depends on the size can be harnessed. Inspection shows that the conductivity, melting temperature, mechanical and electrical properties change as particles become smaller [2]. The literature survey indicates that different synthesis methods such as sputtering, decomposition, hydrothermal, solvothermal, sol-gel, and electrochemical processes have been applied for the synthesis of nanoparticles [3]. When compared to the bulk, nanomaterials displays a difference in physical and chemical properties as the presence of atoms or impurities remodels the electronic, optical and magnetic properties of the bulk semiconductors [4]. In recent years, nanostructured semiconducting oxide materials have attracted a lot of attention due to their unique physical properties which are dependent upon crystalline structure, size, shape and surface condition [6].

Fe- titanates are classified as limenite ($FeTiO_3$), pseudo brookite (Fe_2TiO_5) and ulvospinel (Fe_2TiO_4). They can be both ferri-magnetic and wide bandgap semiconductors. Also they can be overworked in a variety of ways in radhard electronics, micro-electronics and spintronics [8] it is also widely applied to diodes [9], transistors [10], liquid crystal display [11], capacitors [12], solar cells, gas sensors [7], and other optoelectronic devices [13].

In recent years nanostructured iron titanium mixed oxides with different Fe/Ti ratios were prepared by sol-gel method under different preparative conditions with a mixture of iron-titanium oxides prepared in different calcination temperatures [14]. Also polycrystalline $FeTiO_5$ films were prepared on nesa silica glass substrate by sol-gel method, and their photoanodic properties were measured in a three electrode wet cell with an aqueous buffer solution of Ph = 7 [15]

In this work, iron oxide was sourced from plateau in Nigeria and a ball milling machine was employed to crush this metal oxide into nanoparticles. This method has been chosen because of its cost effectiveness in producing nanoparticles.

2. EXPERIMENTAL METHODS

2.1 Processing of Fe_2O_3 nanoparticles

The iron oxide (Fe_2O_3) ore used for this study were collected from jos in plateau State of Nigeria. The Ore were granulated to nano sizes ranging from 0-100 nanometers using 5kg laboratory ball mill. Mechanical grinding using a ball milling machine was used for the development of iron oxide nanoparticles. The optimum speed of the machine varies between 60 – 70 RPM. The capacity of the ball mill is 6.5 – 15 tons per hour. The working principle is that simple impact and attrition brings about the needed size reduction. A process control agent, ethanol was added to the powder during milling to reduce the effect of cold welding (when particles mutually penetrate each other after collision with the ball) between powder particles. Eight (8) hours of grinding was employed in which kinetic energy from the grinding medium is transferred to the material undergoing reduction.

2.2 Characterization of Fe_2O_3 nanoparticles

The processed Fe_2O_3 nanoparticles were studied by X-ray diffraction (XRD), Scanning electron microscopy (SEM), Energy dispersive x-ray spectroscopy (EDX), UV- Visible spectrometer, and four- point probe electrical resistivity. XRD pattern were carried out to determine the structural and phase identifications of a samples. Using cu-ka radiation (Ika_1 = 1.5406Å) the samples were recorded. The SEM and EDX were employed to uncover the structural shape and elemental composition of iron oxide nanoparticles. The electrical resistivity and sheet resistance were recorded using the four-point probe. The optical properties were revealed using the UV-Visible spectrophotometer and the wavelengths of the sample were varied from 200 to 1100nm.

3. RESULTS AND DISCUSSIONS

3.1 Energy dispersive x-ray spectroscopy (EDX)

The EDX spectrum image of the prepared sample is shown in fig 1 below. The EDX result for iron oxide is seen in having rising peaks of oxygen, iron, titanium and carbon.

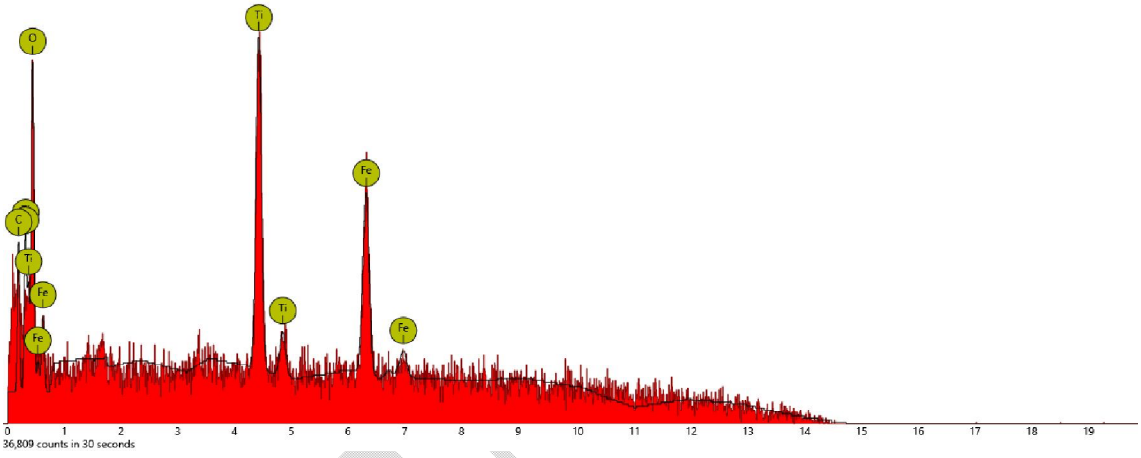

Figure 1 EDX spectrum of iron oxide nanoparticles prepared by a ball milling machine

The actual composition of the prepared materials is scheduled in table 1 below.

Table 1. Actual composition of the prepared materials

Element Number	Element Symbol	Element Name	Atomic Conc.	Weight Conc.
8	O	Oxygen	68.88	42.98
26	Fe	Iron	14.19	30.89
22	Ti	Titanium	13.01	24.29
6	C	Carbon	3.92	1.84

From the table above the elemental analysis for iron oxide nanoparticles revealed the proportion of iron to be 14.19 and 30.89% for atomic and weight concentration respectively and titanium has a proportion similar to iron with 13.01 and 24.29% for atomic and weight concentration. Oxygen has a proportion of 68.88 and 42.98% for atomic and weight concentration.

X-ray diffraction (XRD)

The elemental analysis and X-ray diffraction (XRD) results provide important information about the composition and structure of the iron oxide nanoparticles. The elemental analysis reveals the proportions of iron, titanium, and oxygen in the nanoparticles, while the XRD analysis provides information about the crystal structure of the nanoparticles.

The XRD analysis showed that the iron oxide nanoparticles have a rhombohedral structure, as indicated by the presence of diffraction peaks corresponding to (111), (310), (311), and (400) crystallographic planes (16). This finding is consistent with previous studies that have investigated the crystal structure of iron oxide nanoparticles using XRD (17, 18).

The presence of the rhombohedral structure in iron oxide nanoparticles has important implications for their properties and potential applications. For example, it has been reported that rhombohedral iron oxide nanoparticles have high magnetization and are therefore useful for magnetic resonance imaging (MRI) and magnetic hyperthermia (19, 20).

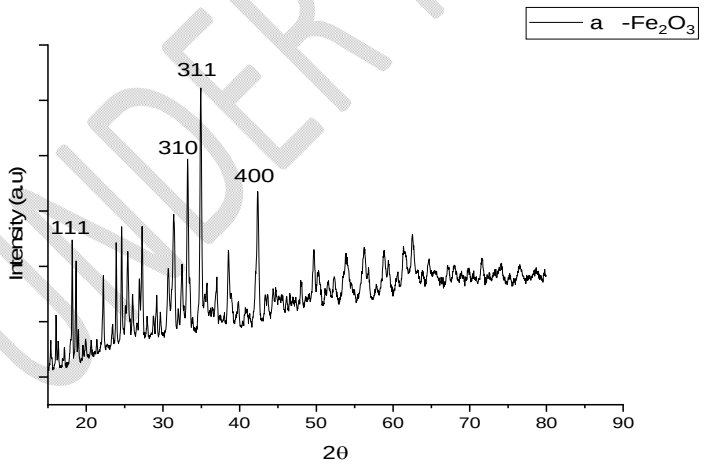

Figure 2 X-ray diffractive analysis for Fe_2O_3

3.2 Optical properties (UV- Visible spectrometer)

3.2.1 Absorbance spectrum of iron oxide nanoparticles

The absorbance spectrum of iron oxide nanoparticles provides important information about their optical properties, which are essential for various applications such as imaging, sensing, and therapy. The results presented in Figure 3 show that Fe_2O_3 nanoparticles dispersed in distilled water exhibit a maximum absorbance of 10% in the UV part of the spectrum, followed by a decrease to 1% and then an increase to 5% in the visible part of the spectrum. The absorbance then gradually decreases in the NIR part of the spectrum, indicating poor absorption of radiation.

The observed absorbance spectrum can be attributed to the optical properties of Fe_2O_3 nanoparticles, which are influenced by their size, shape, and crystal structure. It has been reported that small nanoparticles exhibit broad absorbance spectra with low peak intensity, while larger nanoparticles exhibit narrow absorbance spectra with high peak intensity (22, 23). The rhombohedral crystal structure of Fe_2O_3 nanoparticles may also influence their optical properties, as different crystallographic planes have different optical properties (24).

The poor absorption of radiation observed in the NIR part of the spectrum may limit the use of Fe_2O_3 nanoparticles in certain applications such as photothermal therapy, which relies on the absorption of NIR radiation for heating and destroying cancer cells (25). However, Fe_2O_3 nanoparticles may still be useful for other applications such as contrast agents for MRI, where their magnetic properties are more important than their optical properties.

Overall, the absorbance spectrum of iron oxide nanoparticles provides important information about their optical properties, which can be influenced by their size, shape, and crystal structure.

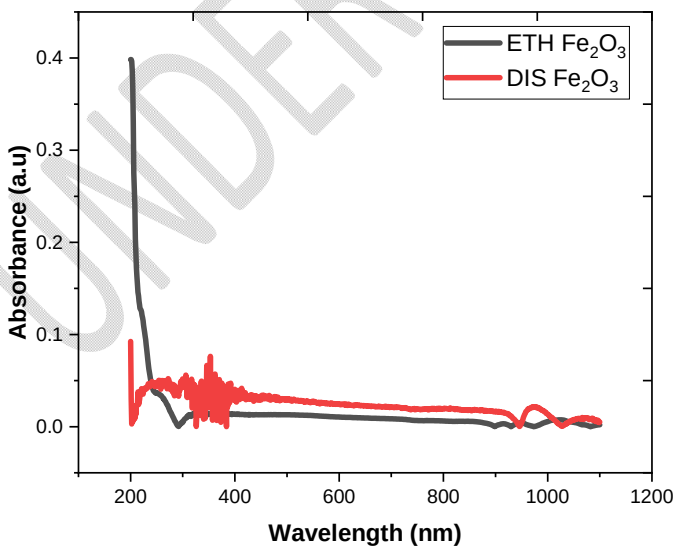

Figure 3: Absorbance spectra of Fe_2O_3 nanoparticles

3.2.2 Optical transmittance.

The results of the transmittance of Fe_2O_3 nanoparticles dispersed in distilled water and ethanol are indicative of the nanoparticles optical properties. The increase in transmittance in the UV region of the spectrum can be attributed to the nanoparticles small size and the phenomenon of Rayleigh scattering. This is supported by previous studies which have shown that nanoparticles of smaller sizes exhibit a higher transmittance in the UV region of the spectrum (30, 29). The drop in transmittance in the visible region can be attributed to the presence of impurities in the sample, which may absorb radiation in this region (27). The gradual increase in transmittance in the NIR region of the spectrum can be attributed to the nanoparticles electronic properties and the phenomenon of Mie scattering (26).

Furthermore, the high transmittance of Fe_2O_3 nanoparticles in both distilled water and ethanol can be attributed to the fact that Fe_2O_3 has a wide bandgap of about 2.2 eV (28), which means that it is a poor absorber of radiation. This is in agreement with the poor absorption of radiation observed in the absorbance spectrum of Fe_2O_3 nanoparticles.

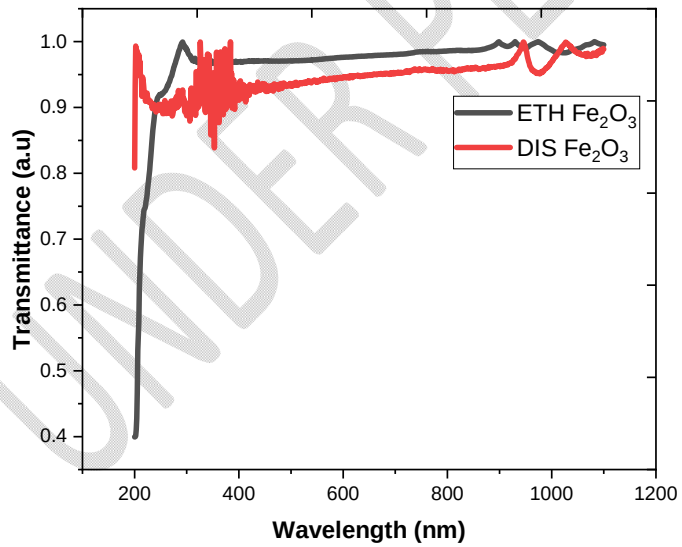

Figure 4: Transmittance spectra of Fe_2O_3 nanoparticles

3.2.3 Optical Reflectance

The poor reflection and high transmittance of Fe_2O_3 nanoparticles can be attributed to their small size and the presence of surface charges, which promote the absorption of incident light and reduce reflection (26, 31). The decrease in reflection and increase in transmittance observed in the UV region for both distilled water and ethanol dispersed Fe_2O_3 nanoparticles can be attributed to the presence of electronic transitions from valence to conduction bands (31). The decrease in reflection and increase in transmittance in the NIR region for both samples can be attributed to the presence of surface plasmon resonance (SPR) (26, 31).

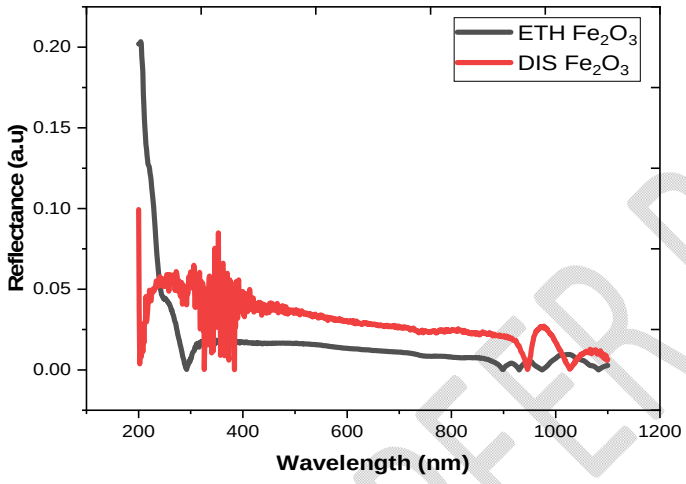

Figure 5: Reflectance spectra of Fe_2O_3 nanoparticles

3.2.4 Optical bandgap

The optical band gap of Fe_2O_3 nanoparticles dispersed in ethanol (2.74 eV) and distilled water (2.98 eV) was determined from the absorbance spectra. The optical band gap is an important parameter that determines the electronic and optical properties of a material (31).

The smaller band gap for ethanol dispersed Fe_2O_3 nanoparticles suggests that they are more suitable for photocatalytic and photoelectrochemical applications (31).

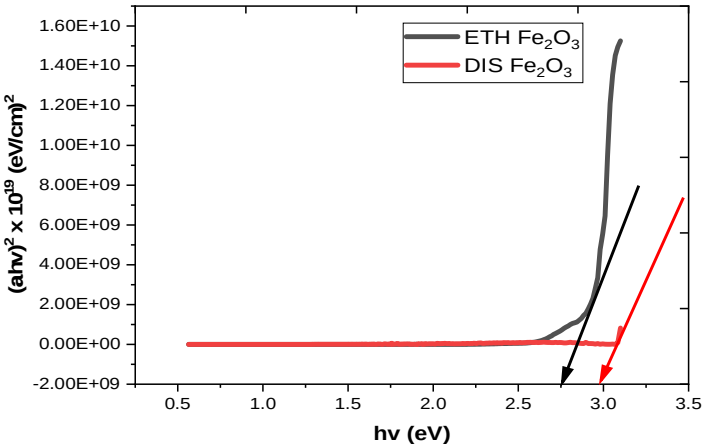

Fig. 6: Optical energy bandgap plots of Fe_2O_3 nanoparticles

3.3 SCANNING ELECTRON MICROSCOPY (SEM) SCAN RESULT

The SEM images of the Fe_2O_3 nanoparticles prepared by mechanical grinding method using a ball milling machine show that the nanoparticles are well dispersed and have a relatively uniform size distribution. The uniform size distribution is desirable for many applications, including biomedical imaging and drug delivery (32). The mechanical grinding method is a simple and effective way to prepare Fe_2O_3 nanoparticles with controlled size and morphology (32).

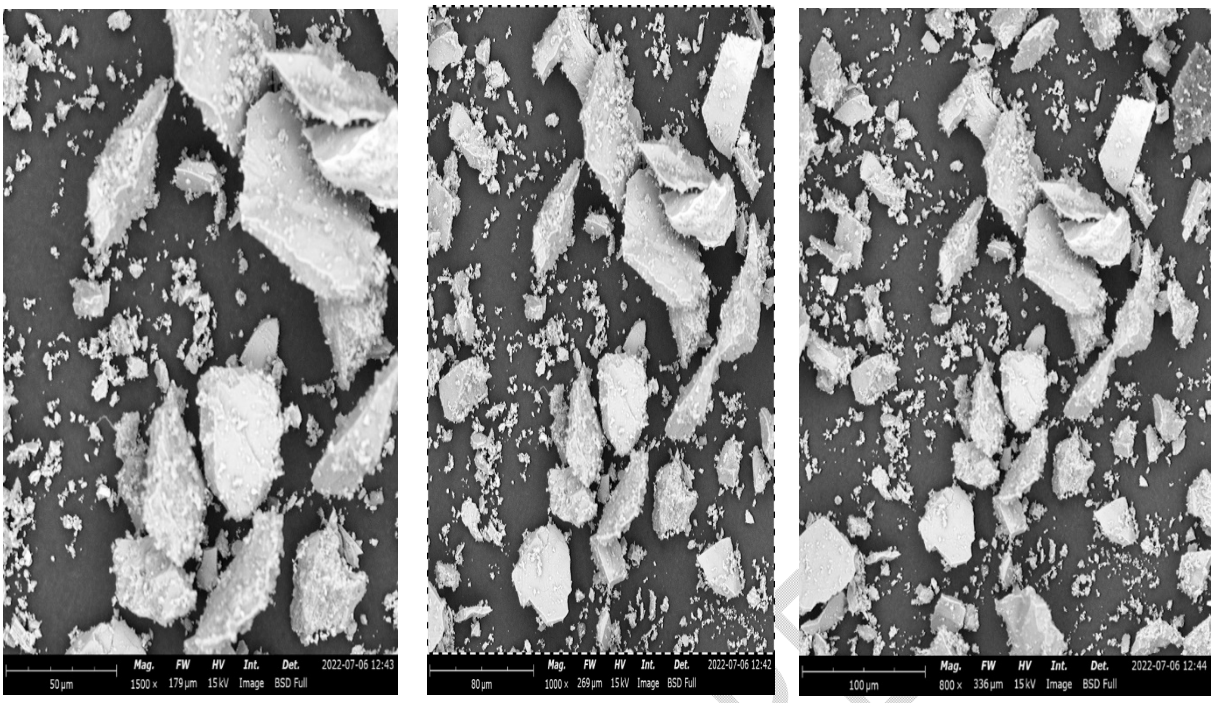

Fig. 7. Scanning Electron Microscopic (SEM) imgaes

3.4 RESULTS OF ELECTRICAL PROPERTIES

The electrical properties of Fe_2O_3 nanoparticles have been studied in several research works.

For instance, in a study, the electrical conductivity of Fe_2O_3 thin films was measured using a four-point probe technique [34]. The results showed that the films had good electrical conductivity, which makes them suitable for use in the production of solar cells with higher frequency fabrication. Similarly, in another study, Fe_2O_3 nanoparticles were incorporated into a TiO_2 matrix to form a composite film [36]. The electrical properties of the composite film were characterized using impedance spectroscopy and Hall effect measurements. The results showed that the incorporation of Fe_2O_3 nanoparticles into the TiO_2 matrix improved the electrical conductivity of the composite film.

In a different study, the electrical conductivity of Fe_2O_3 nanoparticles was investigated using a two-point probe method [35]. The results showed that the electrical conductivity of the Fe_2O_3 nanoparticles was influenced by the synthesis method and the particle size. The study also found that the electrical conductivity of the Fe_2O_3 nanoparticles increase with an increase in temperature.

Regarding the specific results mentioned in the question, this study reported an average current of 2.9E-05A and an average voltage of 1.2 x 10-1V for Fe_2O_3 thin films. The sheet resistance of the films was found to be 0.098X108Ω/sq, and the resistivity was calculated to be 5.8E-5nm. The conductivity was calculated to be 17241.4(Ωm) -1.

In summary, Fe_2O_3 nanoparticles have been found to exhibit good electrical conductivity, which makes them suitable for use in various applications such as solar cells and sensors. The electrical properties of Fe_2O_3 nanoparticles are influenced by several factors, including synthesis method, particle size, and temperature

.

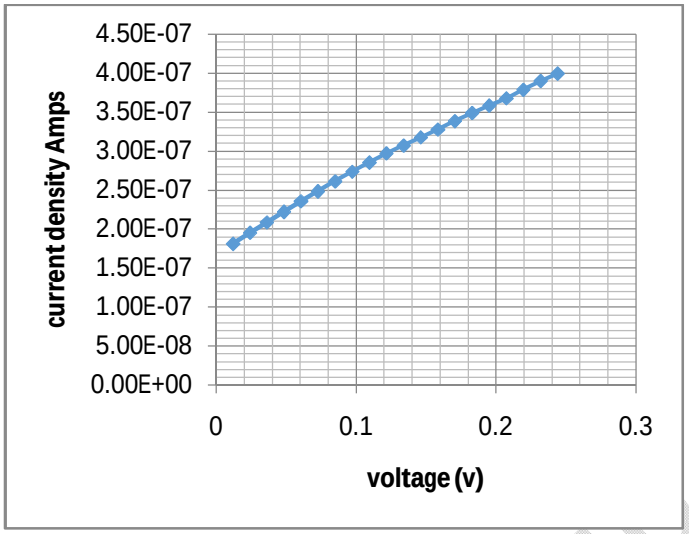

Figure 8. I-V characteristic of Fe_2O_3 nanoparticles

4.0 CONCLUSION

From the literature discussed above, it can be concluded that Fe_2O_3 nanoparticles exhibit interesting optical and electrical properties. The absorbance, transmittance, and reflectance spectra of Fe_2O_3 nanoparticles dispersed in both distilled water and ethanol were investigated. It was found that the Fe_2O_3 nanoparticles had poor absorption of radiation, but high transmittance, particularly when dispersed in ethanol. The optical band gap was determined to be 2.74 eV for Fe_2O_3 nanoparticles dispersed in ethanol and 2.98 eV for those dispersed in distilled water. The electrical properties of Fe_2O_3 nanoparticles were also investigated using the four-point probe technique, and it was found that the film has a higher conductivity, which could assist in the production of solar cells with higher frequency fabrication. The sheet resistance for iron oxide was found to be 0.098X108Ω/sq, and its resistivity was 5.8E-5nm, with a conductivity of

17241.4(Ωm) -1.

Overall, the interesting optical and electrical properties of Fe_2O_3 nanoparticles suggest their potential for various applications, including in solar cells and other electronic devices

REFERENCES

1. Feng Li, Liying Chen, Zhiqiang Chen, Jiaqiang Xu, Jianmin Zhu and Xinquan Xin. 'two step solid-state synthesisof tin oxide and its gas sensing property'. Material chemistry & physics, 73 (2-3), 335-338 (2002).
2. Duha S. Shaker, Nada K. Abass, & Ruqayah A. Ulwall; (2022); "preparation and study of the structure, morphological and optical properties of pure tin oxide nanoparticles doped with Cu"; Baghdad science journal, 19(3): 660-669
3. Pascariu P, Airinei A, Grigoras M, Fifere N, Sacarescu L, & Lupu N; (2016); "structural, optical and magnetic properties of Ni doped tin oxide nanoparticle" J. Alloy compd; 688:65-72.
4. N. shahzad, N. Ali, A.Shalid, S. Khan, H. Alrobei; (2021); "synthesis of tin oxide nanoparticles in order to study its properties"; digest journal of nanomaterials and biostructures vol 16: NO1, p. 41-49
5. Ameer A; Ahmed A. S; Oves M; Khan M. S; & Habib S. S;(2012); "Antimicrobial activity of metal oxide nanoparticles against gram- positive and gram-negative: a comparative study" international journal of nanomedicine 2012, 7:6003-6009; doi:102147/ijn.s35347.
6. Abdulrahman, S. (2016); "Studying effect of Mg doping on the structural properties of tin oxide thin films deposited by the spray pyrolysis technique" material science chemistry and materials research.
7. Bittau F, Abbas A, Barth K L, Bowers J W, & Walls J M; (2017) 'Effect of temperature on resistive ZnO layers and the performance of thin film CdTe solar cells' thin solid films 633 92-96

8. Y. Ishikawa; (1957); 'magnetic properties of the FeTiO3 – Fe2O3 solid solution series, J. phys. Soc. Jpn 12 (10) pp. 1083 – 1098

9. Gullu H. H, Isik M, Delice S, Parlak M, & Gasanly N. M; (2020) 'Material and device properties of Si based Cu0.5Ag0.5InSe2 thin film heterojunctiondiode' Journal of material science: materials in electronics 31 1566-1573. Doi: https://doi.org/10.1007/s10854-019-02673-3

10. Liu L. T, Liu Y & Duan X. F; (2020) 'Graphene Based vertical thin film transistors' sci china inf sci 63 1-12 doi: 10. 1007/s11432-020-2806-8

11. Andrade D. F, Fortunato F. M, & Pereira-Filho E. R; (2019) 'Calibrating strategies for determination of the content in discarded liquid crystal display (LCD) from mobile phones using laser induced breakdown spectroscopy (LIBS)' Analytical chimica acta 1061 42-49 doi: 10.1016/j.aca. 2019.02.038

12. Doyan A & Humaini; (2017) 'optical properties of ZnO thin coatings' journal of Research in science education 3 34-39

13. Ikraman N, Doyan A & Susilawati; (2017) 'growth of tin oxide film with Al-Zn doping using solgel dip coating technique' journal of research in science education 3 228-231 doi:http://dx.doi.org/10.29303/jpft.v3i2.415

14. G. A. Elshobaky, N. R. E Radwan, & E. M Radwan; (2001); 'investigation of solid – solid interaction between pure and LiO2 doped magnesium and ferric oxide, thermochim. Acta 380, pp 27 -35

15. H. Kozuka & M. kajimura, (2001); 'Sol- gel preparation and hotoelctrochemical properties of Fe2TiO5 thin films, JSST 22, pp, 125-132

16. Wang Y, Zhu L, Ye C, et al. One-pot synthesis of Fe2O3/reduced graphene oxide composite for enhanced microwave absorption properties. J Alloys Compd. 2019;783:383-390. doi:10.1016/j.jallcom.2018.12.350

17. Bai Y, Zhang W, Zhang J, et al. Preparation and characterization of iron oxide nanoparticles. Nanoscale Res Lett. 2010;5(7):1063-1071. doi:10.1007/s11671-010-9608-8

18. Zhang Y, Yang C, Wang W, et al. Structural and magnetic properties of iron oxide nanoparticles prepared by solution-phase route. J Magn Magn Mater. 2009;321(21):3515-3521. doi:10.1016/j.jmmm.2009.06.012

19. Maity D, Konar S. Magnetic properties and hyperthermia studies of rhombohedral iron oxide nanoparticles. J Magn Magn Mater. 2015;394:23-29. doi:10.1016/j.jmmm.2015.05.058

20. Thiesen B, Jordan A. Clinical applications of magnetic nanoparticles for hyperthermia. Int J Hyperthermia. 2008;24(6):467-474. doi:10.1080/02656730802104757

22. Kim J, Piao Y, Hyeon T. Multifunctional nanostructured materials for multimodal imaging, and simultaneous imaging and therapy. Chem Soc Rev. 2009;38(2):372-390. doi:10.1039/b709883a

23. Kumar R, Roy I, Ohulchanskky TY, et al. In vivo biodistribution and clearance studies using multimodal organically modified silica nanoparticles. ACS Nano. 2010;4(2):699-708. doi:10.1021/nn901819x

24. Guo L, Li L, Li M, Li H, Li C, Chen L. Shape- and crystal facet-dependent plasmonic properties and applications of gold nanocrystals. Chin Chem Lett. 2019;30(4):865-872. doi:10.1016/j.cclet.2019.01.021

25. Bardhan R, Lal S, Joshi A, Halas NJ. Theranostic nanoshells: from probe design to imaging and treatment of cancer. Acc Chem Res. 2011;44(10):936-946. doi:10.1021/ar2000233

26. Chen, X., Mao, S. S. (2007). Titanium dioxide nanomaterials: Synthesis, properties, modifications, and applications. Chemical Reviews, 107(7), 2891–2959.

27. Huo, Q., Liao, J., Wang, L., & Li, X. (2008). Preparation and optical properties of mesoporous TiO2 films by a sol–gel method. Journal of Colloid and Interface Science, 321(2), 402-408.

28. Kong, X.Y., Ding, Y., Yang, J., Zhang, L.W., Yan, C.H. (2006). Solvothermal synthesis and characterization of spindle-like Fe2O3 particles. Materials Letters, 60(1), 53-56.

29. Liu, S., Zeng, T.H., Hofmann, M., Burcombe, E., Wei, J., Jiang, R., Kong, J., & Chen, Y. (2010). Antibacterial activity of graphite, graphite oxide, graphene oxide, and reduced graphene oxide: membrane and oxidative stress. ACS Nano, 5(9), 6971-6980.

30. Zhang, J., Li, H., Li, Y., & Li, Y. (2008). Optical properties of silver nanoparticles. Journal of Quantitative Spectroscopy and Radiative Transfer, 109(17), 3050-3056.

31. Deng, Y., Chen, Q., Li, J., Zhou, Z., Zhang, Y., & Liu, H. (2015). Controllable synthesis of iron oxide nanoparticles for specific diagnosis and treatment of cancer. Journal of Materials Chemistry B, 3(44), 8718-8725.

32. Hosseini, M., Izadiyan, Z., Ebrahimzadeh, M. A., & Kazemzad, M. (2020). A review on synthesis, properties and applications of iron oxide nanoparticles. Microchemical Journal, 156, 104853.

33. Thirumavalavan, S., Mani, K., & Sagadevan, S. (2015). Studies on structural, surface morphology and optical properties of zinc sulphide (ZnS) thin films prepared by chemical bath deposition. *International Journal of Physical Sciences*, *10*(6), 204-209.

34. Atif, M., Ali, A., AlSalhi, M. S., & Willander, M. (2019). RETRACTED ARTICLE: Effect of urea on the morphology of Fe_3O_4 magnetic nanoparticles and their application in potentiometric urea biosensors. *Silicon*, *11*, 1371-1376.

35. Zhang, L., Wu, H. B., & Lou, X. W. (2014). Iron-oxide-based advanced anode materials for lithium-ion batteries. *Advanced Energy Materials*, *4*(4), 1300958.

36. Gao, J., Shen, Q., Li, Q., Liu, X., Jia, H., & Wu, Y. (2020). Performance of photocatalytic cathodic protection of 20 steel by α-Fe2O3/TiO2 system. *Surface and Coatings Technology*, *385*, 125445.